Science Advances
AAAS

advances.sciencemag.org/cgi/content/full/5/6/eaax2650/DC1

Supplementary Materials for

Structure of the saxiphilin:saxitoxin (STX) complex reveals a convergent molecular recognition strategy for paralytic toxins

Tien-Jui Yen, Marco Lolicato, Rhiannon Thomas-Tran, J. Du Bois, Daniel L. Minor Jr.*

*Corresponding author. Email: daniel.minor@ucsf.edu

Published 19 June 2019, *Sci. Adv.* **5**, eaax2650 (2019)
DOI: 10.1126/sciadv.aax2650

The PDF file includes:

Other Supplementary Material for this manuscript includes the following:

(available at advances.sciencemag.org/cgi/content/full/5/6/eaax2650/DC1)

Movie S1 (.mp4 format). Sxph conformational changes upon STX binding.

Table S1. Crystallographic data collection and refinement statistics.

	apo-Saxiphilin	Sxph:STX complex (soaked)	Sxph:STX complex (co-crystal)
Data Collection			
Space group	$P2_12_12_1$	$P2_12_12_1$	$P2_12_12_1$
Unit cell			
a, b, c (Å)[a]	96.2, 111.3, 254.8	96.4, 110.8, 254.6	96.6, 111.7, 254.6
α, β, γ (°)	90, 90, 90	90, 90, 90	90, 90, 90
Resolution (Å)	48.2-2.50 (2.54-2.50)	48.2-2.50 (2.54-2.50)	48.3- 2.12 (2.16-2.12)
Total reflections	1143210	1155387	1962129
Unique reflections	95268	94650	156355
Completeness (%)	99.8 (97.3)	99.6 (95.2)	99.9 (98.5)
Redundancy	12.0 (6.6)	12.2 (6.7)	12.5 (7.4)
I/σI	16.0 (1.1)	14.7 (0.5)	13.3 (0.3)
$CC_{1/2}$	1 (0.57)	1 (0.25)	1 (0.10)
Refinement [b]			
R_{work} (%)	22.4	23.7	23.8
R_{free} (%)	25.3	26.2	25.9
RMS deviations			
Bonds (Å)	0.003	0.003	0.002
Angles (°)	0.68	0.76	0.68
Average B factor	83.3	105.0	94.2
Protein	83.6	105.1	94.6
Water	59.5	69.7	69.4
Ligand	-	116.1	95.1
Ramachandran [%]			
Allowed/generous/disallowed	95.2/4.0/0.8	93.8/5.0/1.2	95.3/3.6/1.1

[a] statistics for the highest resolution shell are shown in parentheses.

[b] Final refined models cover all residues except for the following:

apo-Saxiphilin

Chain A, 171-178, 289, 571-573, 620, and 637-646

Chain B, 1-4 and 169-178

Sxph:STX complex (soaked)

Chain A : 1-3, 172-177,585-586, 620-621, 637-647, 673-674, 701-711, and 717-718

Chain B: 1-4, 169-179, and 572-573

Sxph:STX complex (co-crystal)

Chain A : 1,2, 171-173, 585-586, 620-621, 637-647, 673-674

Chain B: 1-4, 169-178, and 572-573

Fig. S1

Yen *et al.*

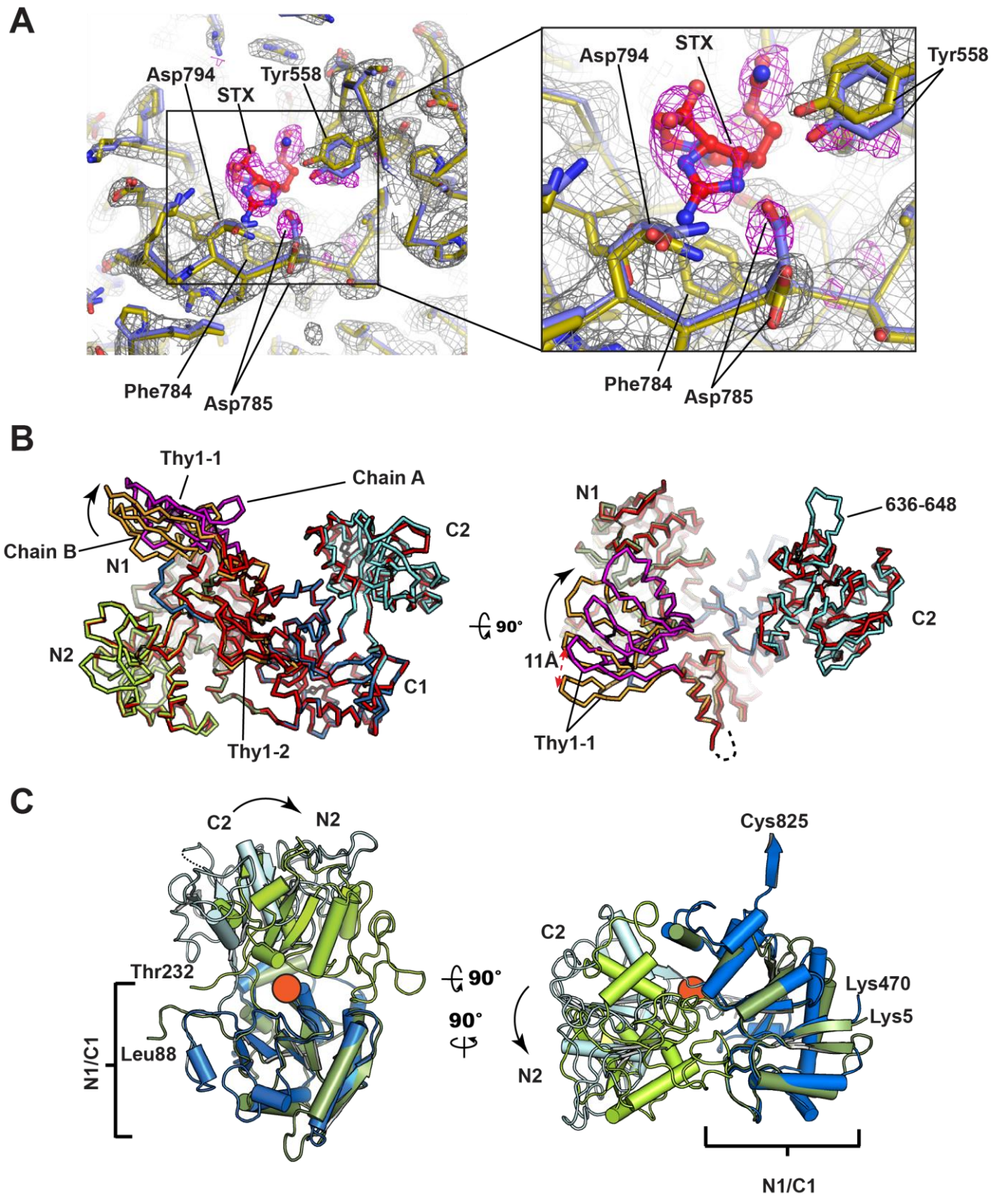

Fig. S1. Sxph structural analysis. (**A**) Exemplar 2Fo-Fc electron density (1.5σ)(grey) and Fo-Fo (5σ)(magenta) for Sxph and STX, respectively. Sxph (olive) and Sxph:STX (marine) are shown and select residues are labeled. STX is red. (**B**) Ribbon diagram superposition of apo-Sxph Chain A (red and magenta) and Chain B ($RMSD_{C\alpha}$ = 0.61 Å over 663 residues). Chain A Thy1-1 is colored magenta. Chain B subdomains are colored: N1 (smudge), N2 (Limon), Thy (bright orange), C1 (marine), and C2 (cyan). Relative displacement of the Thy1-1 is indicated. (**C**) Superposition of apo-Sxph N-lobe (N1, smudge; N2, limon) and C-lobe (C1, marine; C2, cyan). Relative motions of N2 and C2 subdomains are indicated. As a point of reference, the orange sphere marks position that corresponds to the transferrin Fe^{3+} binding site. The N-lobe and C1 cores have lowest B-factors (average B factor of 74.0 $Å^2$ for N-lobe and 63.4 $Å^2$ for C1 domain), whereas the majority of C2 is more mobile (average B-factor of 108.4 $Å^2$).

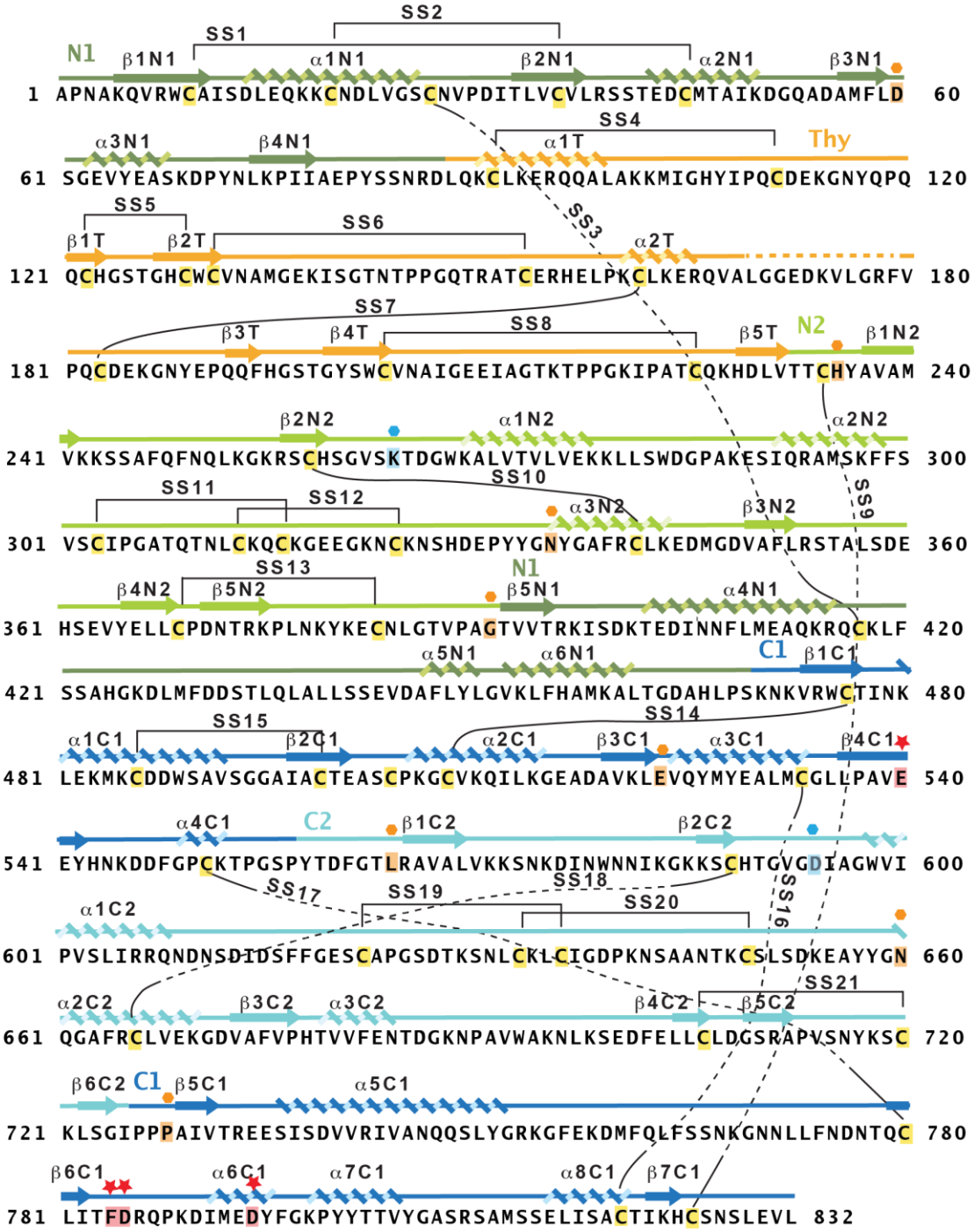

Fig. S2. Sxph sequence, secondary structure, and disulfide map. *Rana catesbeiana* Sxph sequence. Secondary structures are indicated. Domains are labeled and colored as in fig. S1A. Cysteine residues (yellow) and disulfide bonds (SS#) are indicated. Residues corresponding to transferrin Fe^{3+} and carbonate ligands are indicated by orange and blue hexagons, respectively and highlighted. Residues corresponding to STX-interacting residues are indicated by the red star and are highlighted.

Fig. S3

Yen *et al.*

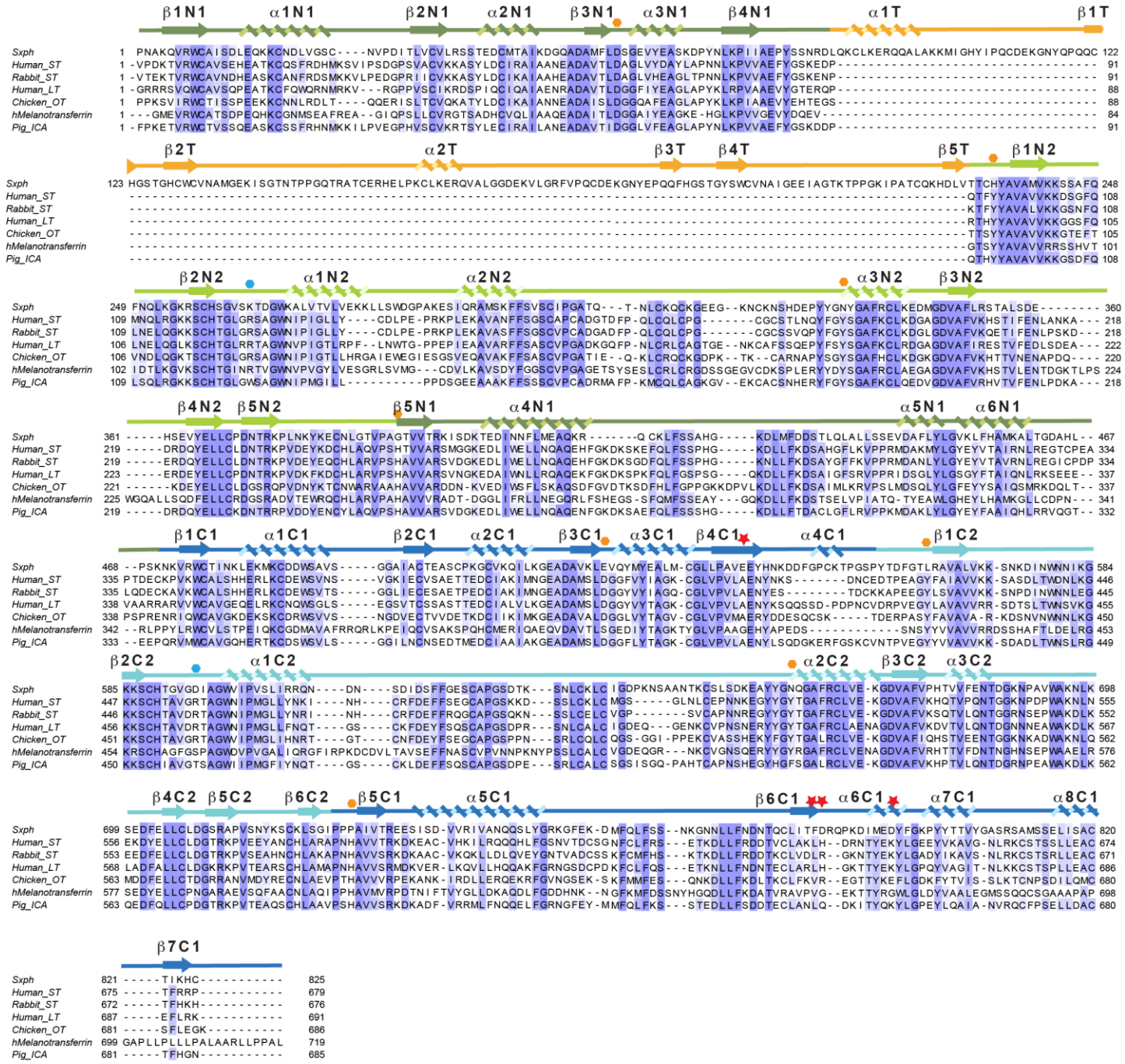

Fig. S3. Comparison of Sxph and representative transferrin family member sequences.

Sequence alignment of *Rana catesbeiana* Sxph with representative members of the transferrin family. Human serum transferrin (Human_ST) (UniProtKB: P02787), rabbit serum transferrin (Rabbit_ST) (UniProtKB:P19134), human lactotransferrin (Human_LT) (UniProtKB:P02788), chicken ovotransferrin (Chicken_OT) (UniProtKB:P02789), human melanotransferrin (Melanotransferrin) (UniProtKB:P08582), and pig inhibitor of carbonic anhydrase (Pig_ICA) (UniProtKB:Q29545). Sxph

domain and secondary structures are indicated and colored as in fig. S1B. Residues corresponding to transferrin Fe^{3+} and carbonate ligands are indicated by orange and blue hexagons, respectively and highlighted (*38*).

Fig. S4 Yen *et al.*

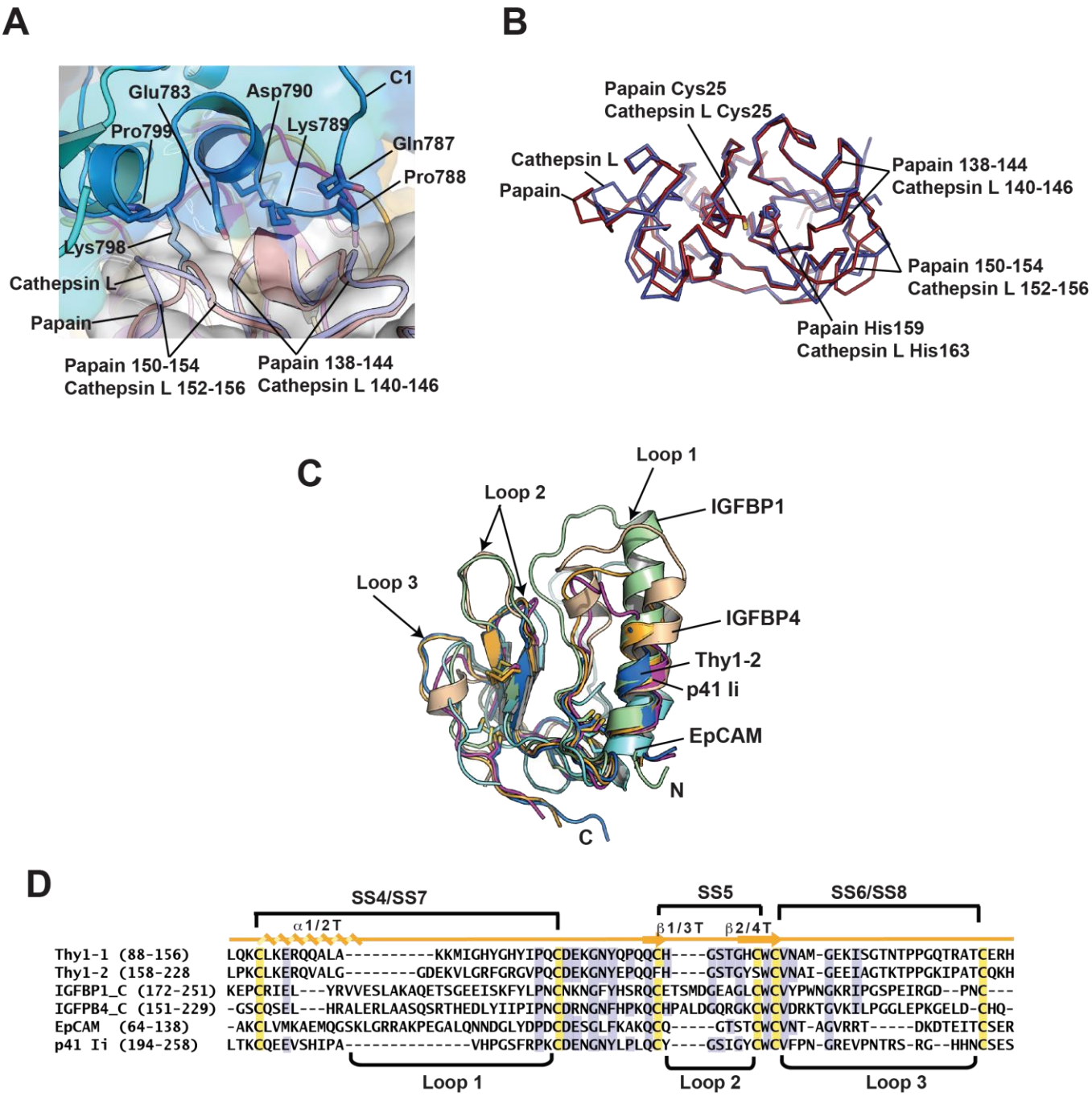

Fig. S4. Sxph thyroglobulin domain structural analysis. (**A**) Close up view of the superposition of the Sxph Thy1-2 domain on the p41 Ii:cathepsin L complex and papain (PDB: 1POP) (*68*) on the p41:cathepsin L complex (PDB: 1ICF) (*38*). Sxph residues that clash with the enzyme surface are labeled. Regions of cathepsin L (light blue) and papain (firebrick) are indicated. (**B**) Superposition of cathepsin L from the p41 Ii:cathepsin complex (PDB: 1ICF) (*38*) and papain (PDB: 1POP) (*68*). $RMSD_{C\alpha}$ = 0.66 Å over 168 residues. Active site residues and regions of clash from panel '**A**' are indicated and clash with Sxph C1 residues 787-790, 783, and 787-799. (**C**) Superposition of Thy1

domains from Sxph (Thy1-1, bright orange, Thy1-2, marine), p41 (1ICF, magenta) (*38*), IGFBP1 (1ZT3, green) (*69*), IGPBP4 (PDB: 2DSR, wheat)(*70*), and EpCAM (PDB: 4MZV, aquamarine)(*71*). (**D**) Sequence comparison of Thy1 domains from 'C'. Secondary structure elements and disulfide bond labels are from the Sxph Thy1 domains.

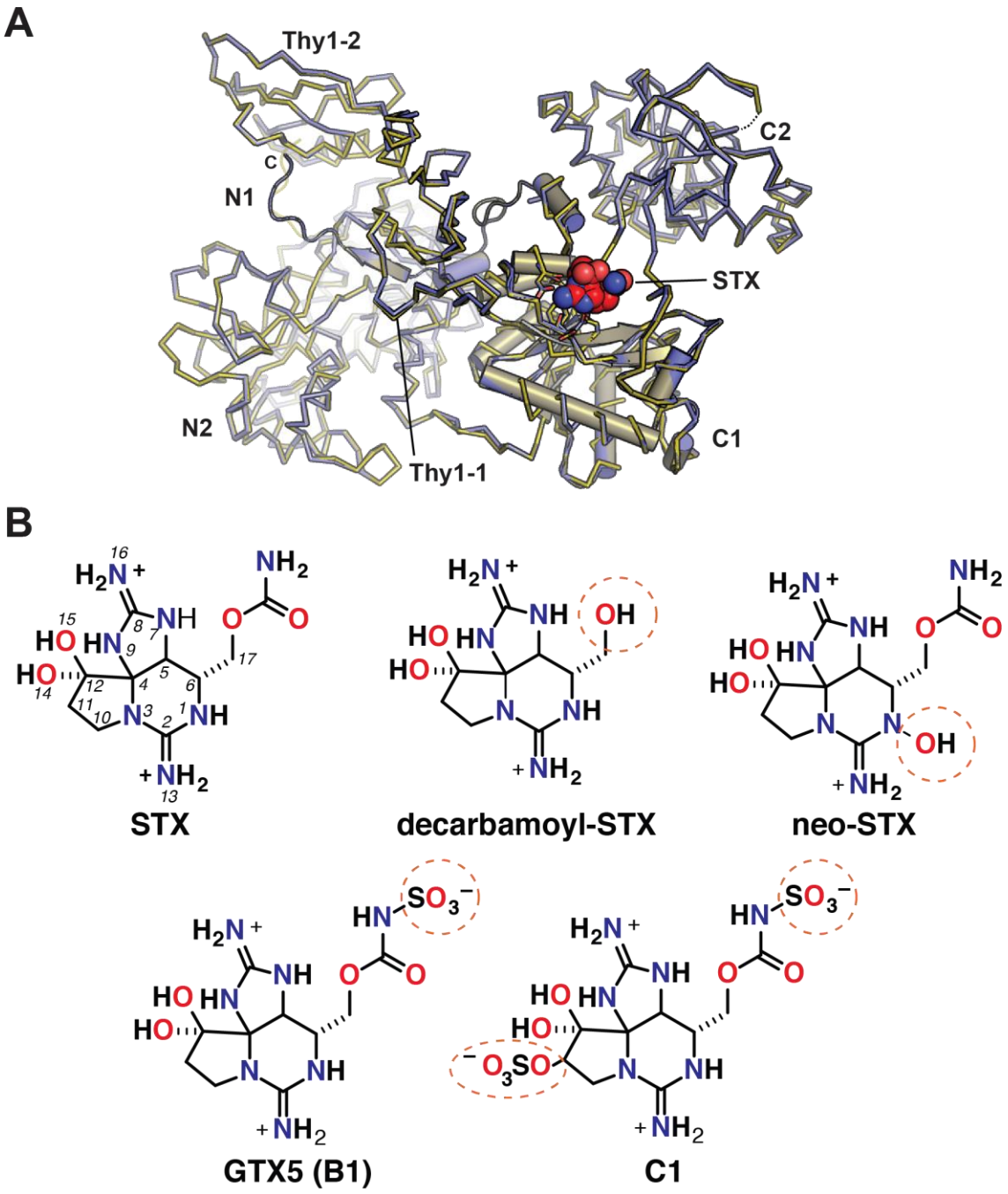

Fig. S5. STX-binding site and STX derivatives. (**A**) Superposition of apo-Sxph (olive) and STX bound STX (slate) shown as ribbons ($RMSD_{C\alpha}$ = 0.21 Å over 671 residues). C1 domain is also shown in cartoon representation. STX (red) is shown as space filling. Residues in the STX binding site are shown as sticks. (**B**) STX and derivatives. STX atom numbering is shown in italics. Dashed circles indicate sites of modification in STX derivatives. Gonyautoxin 5 is also known as 'B1'.

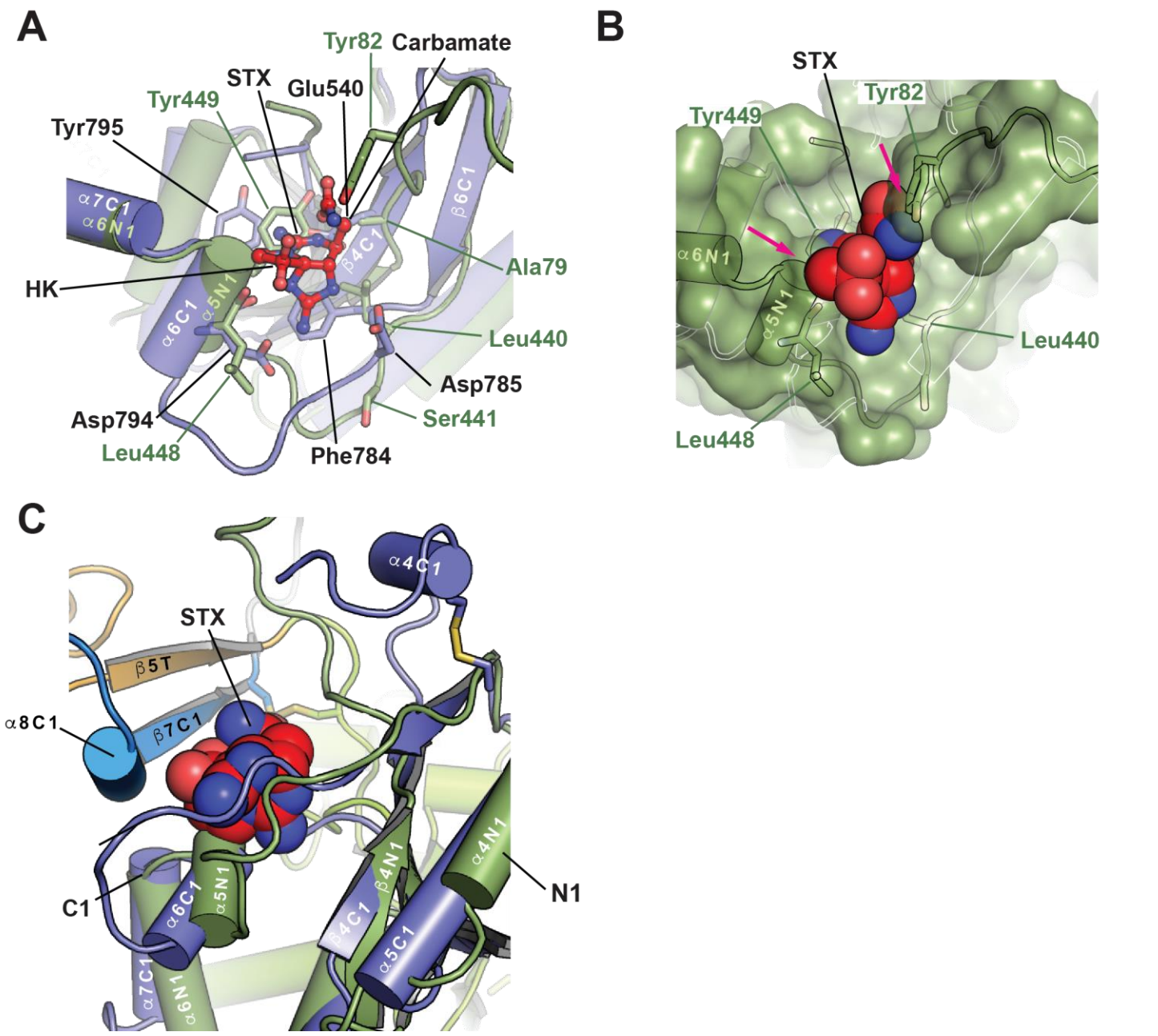

Fig. S6. Structural comparison of Sxph N1 and C1 domains. (**A**) Superposition of the Sxph N1 (green), and C1 (slate) domains ($RMSD_{C\alpha}$ = 0.90 Å over 86 residues). STX is shown in red. N1 domain residues corresponding to C1 domain STX binding residues are shown as sticks and are labeled. (**B**) Surface rendering of the Sxph N1 proto-pocket (green). STX is shown in space-filling representation. Magenta arrows indicate clash sites. (**C**) Superposition Sxph N1 (green), and C1 (slate) domains. Elements from Sxph that occlude the N1 domain proto-pocket are labeled with black letters. STX (red) is shown in space filling representation.

Fig. S7

Yen *et al.*

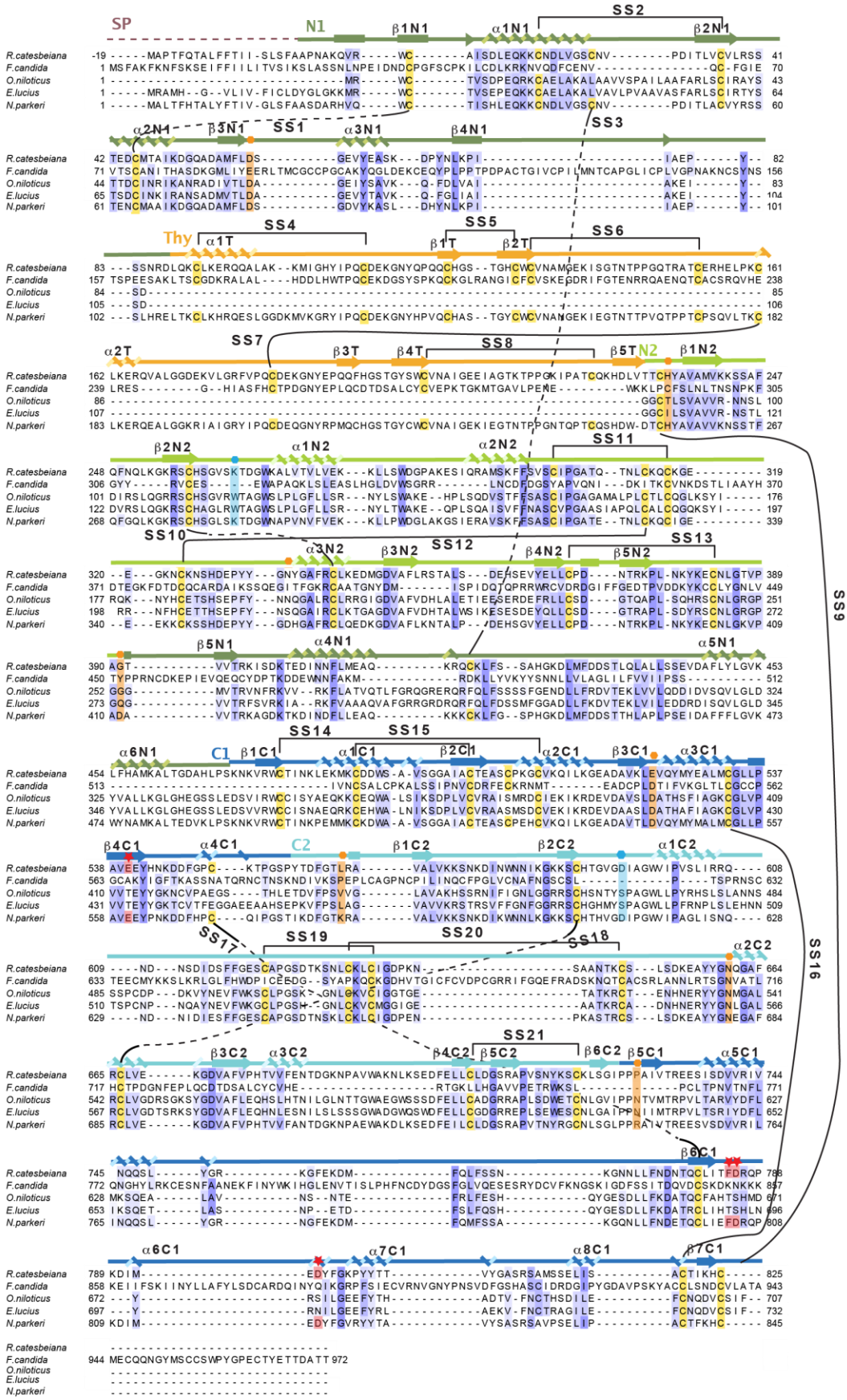

Fig. S7. Sequence comparison of Sxph and putative Sxph homologs. Sequence alignment of *Rana catesbeiana* Sxph with putative Sxph homologs from springtail (*Folsomia candida*) (NCBI: OXA56246.1), Nile tilapia (*Oreochromis niloticus*) (NCBI:XP_019214738.1), Northern pike (*Esox lucius*) (NCBI:XP_010879337.1), and High Himalaya frog (*Nanorana parkeri*) (NCBI: XP_018410833.1).

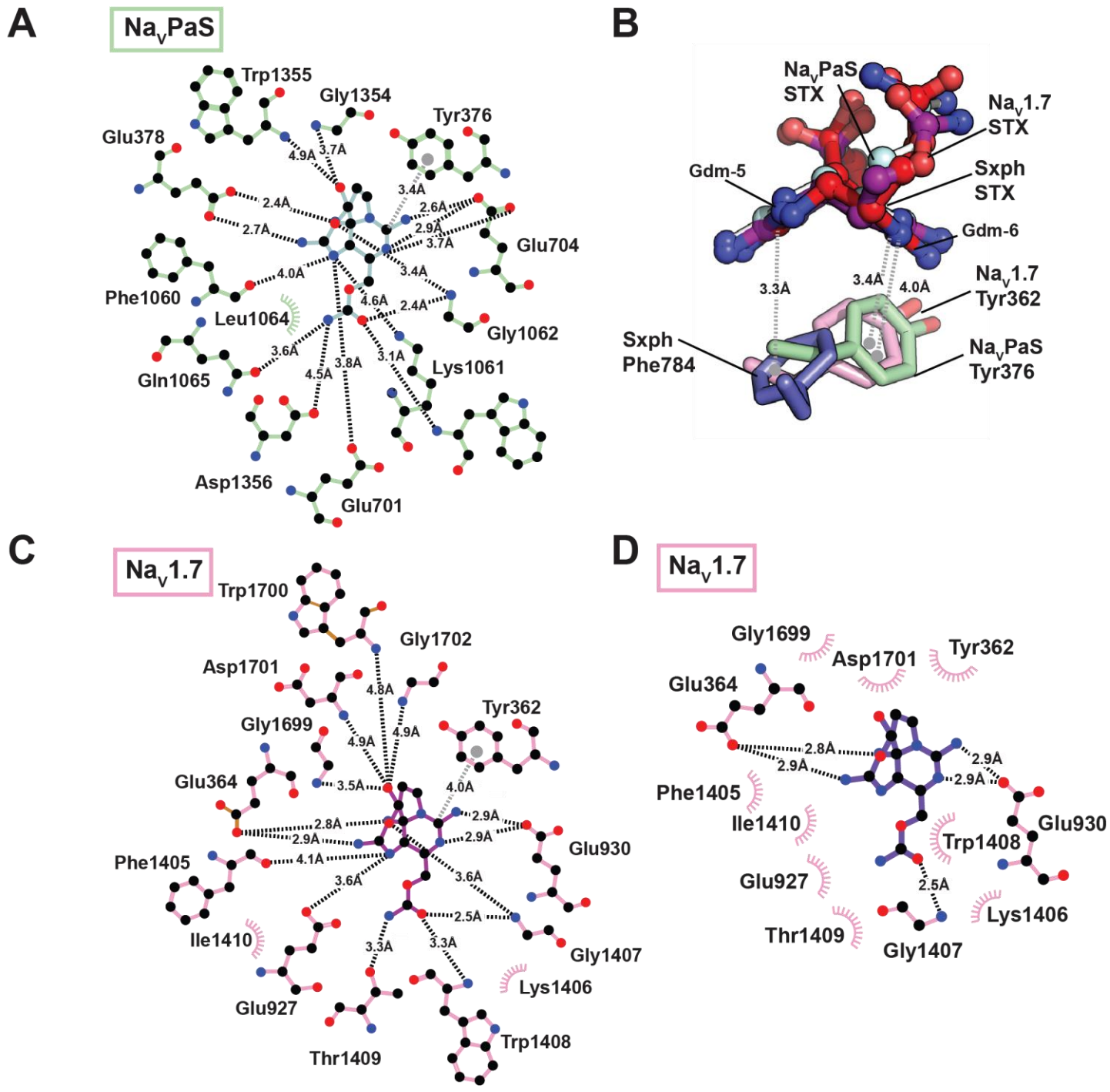

Fig. S8. Na_VPaS:STX and $Na_V1.7$:STX interactions. (**A**) Na_VPaS:STX interactions (PDB 6a91)(*29*) determined with LIGPLOT (*67*) and a cutoff of 5.0 Å. (**B**) Comparison of STX cation-π interactions with Sxph (blue), Na_VPaS (green), and Na_V1.7 (magenta). STX from the Sxph:STX complex (red), Na_VPaS:STX complex (cyan), and Na_V1.7:STX complex (violet) are indicated. (**C** and **D**) Na_V1.7:STX

interactions (PDB:6J8G) (*47*) determined with LIGPLOT (*67*) a cutoffs of 5.0 Å and 3.35Å, respectively.

Movie S1. Sxph conformational changes upon STX binding. Morph between the apo-Sxph and Sxph:STX structures showing the STX binding pocket. Select sidechain and backbone atoms are shown as sticks. STX is shown as red sticks.